Sustainable Energy & Fuels

Cost estimates of production scale semitransparent organic photovoltaic modules for building integrated photovoltaics.

Journal:	*Sustainable Energy & Fuels*
Manuscript ID	SE-ART-06-2020-000910.R1
Article Type:	Paper
Date Submitted by the Author:	08-Sep-2020
Complete List of Authors:	Lee, Byungjun; University of Michigan, EECS Lahann, Lucas; University of Michigan, EECS Li, Yongxi; University of Michigan Forrest, Stephen; University of Michigan, EECS

Cost estimates of production scale semitransparent organic photovoltaic modules for building integrated photovoltaics.

Byungjun Lee[1], Lucas Lahann[1], Yongxi Li[1], and Stephen R. Forrest[1,2]

[1]Department of Electrical Engineering and Computer Science, University of Michigan

[2]Departments of Physics and Materials Science and Engineering, University of Michigan, Ann Arbor, MI

Abstract

Building integrated photovoltaics (BIPVs) are attached to commercial and residential structures to enable solar energy harvesting. While conventional Si photovoltaics (PVs) are dominant in the current market, second and third generation thin film solar cells based on amorphous Si, CdTe, CIGS, perovskites or organic photovoltaics (OPVs) are often considered as an alternative for BIPV applications since they may offer reduced costs compared to Si PVs. Indeed, recent advances in performance suggest that lightweight, flexible and visibly transparent OPVs can potentially be integrated into windows or other applications to which Si PVs are less well suited. Here, we estimate the cost of high efficiency, semitransparent OPVs (ST-OPVs) based on solution processing in a roll-to-roll (R2R) manufacturing line. Assuming modules with 10% power conversion efficiency (*PCE*), a 70% geometric fill factor (*GFF*), and 95% inverter efficiency, we anticipate a \$1.6/W_p module manufacturing cost that includes the cost of the microinverter to condition the OPV dc output to be compatible with the ac line voltage of the building. The materials and inverter cost comprise ~90% of the total module cost. Hence, with simplified material synthesis and a lower inverter cost, including marginally improved *PCE* and *GFF*, we expect the cost can be as low as \$0.47/W_p. While the module costs ~60% of the average (uninstalled) double-pane window, we expect the payback period can be as short as 2 to 6 years, suggesting that OPVs can be an economic and attractive candidate for BIPV applications.

I. Introduction

Building integrated photovoltaics (BIPVs) are a space-efficient means for harvesting solar energy by replacing or covering a part of a building (e.g. rooftop, façade or windows) with photovoltaic modules.[1]–[4] More than 80% of the current BIPV market is based on rooftop installed crystalline Si (c-Si) modules, with the remaining 20% installed mostly on façades.[4], [5] Integration of c-Si photovoltaics onto windows, however, has the disadvantage of visible opacity,[6], [7] requiring that the cells be perforated with holes, or applied in strips. Both strategies result in a reduction in their geometric fill factor (*GFF,* is the ratio of active cell to total module area), and hence limit the power that can be produced. An alternative approach is to employ visibly semitransparent photovoltaics based on organic semiconductors, quantum dots and perovskites integrated onto windows.[1]–[3], [8]–[10] However, besides organic semiconductors, application of such materials in BIPV systems has not been reported due to inadequate device performance and reliability, limited scalability, toxicity of materials, or high manufacturing cost compared to c-Si photovoltaics.[1], [2] Despite the scalability and successful demonstration of display manufacturing on an enormous scale, organic semiconductors are often considered to be an immature alternative to c-Si PVs within the BIPV industry.[1], [2] Recently, organic photovoltaic cells (OPVs) based on DBP:C_{70} with accelerated intrinsic lifetimes extending to T_{80} = 27000 yr have been reported,[11] where T_{80} is a time of operation for the *PCE* to drop to 80% of its initial value. Furthermore, OPVs with cell *PCE* > 17% ,[12] module *PCE* > 14%[13] and neutral density, semi-transparent OPVs (ST-OPVs) with *PCE* > 10% have been reported. [14]

The visible transmittance of the ST-OPV cell is another important metric determining how well the technology is suited for use in power generating windows. To define transparency of the device, the average visible transmittance (*AVT*) which is the arithmetic mean of transmittance of the cell from 400 to 650 nm is often used. However, a more apt comparison that quantifies the *appearance* of the sunlight entering an interior space is provided by average photopic transmittance (*APT*), which is the transmittance of the cell weighted by the spectral response of human eye to a window illuminated by an AM 1.5G reference spectrum. Then, the light utilization efficiency (*LUE*), which is the product of *PCE* and *APT,* combines these factors into a ST-OPV figure of merit.[15], [16] A compilation of the *LUE* vs. *APT* for a range of thin film technologies (including amorphous Si – a-Si – perovskites, and OPVs) originally summarized by Lunt *et al*.[16] and updated by Li *et al*. [15] is provided in Fig. 1, and device performance of highlighted results are shown in Table I. Apparently, ST-OPVs have the highest combination of transparency and efficiency, with a maximum *LUE* = 5%, compared with other thin film solar cell technologies. Given the scalability of OPVs using printing or other roll-to-roll (R2R) manufacturing processes, [17]–[19] and their possibility for exceptionally long operational lifetimes,[11] these advances point to their particular suitability for BIPV applications, especially for semi-transparent power generating windows.

Beyond these promising studies of laboratory cell performance, the acceptability of a PV technology ultimately hinges on the cost to produce large scale modules at high volume. Several different estimates of OPV module cost have varied from \$0.2 to \$1.2/W_p based on differing assumptions of materials sets employed, and on module efficiencies that range from 5-10%.[20]–[24] Up until now, however, most cost analyses are based on opaque cells while also omitting the costs of inverters, and miscellaneous costs such as sales, administrative, marketing, and R&D. Furthermore, they do not consider recent significant advances in OPV technology that have occurred over the last few years. In this work, we estimate manufacturing cost of *semitransparent*

OPV modules based on assumptions and accuracy corresponding to Class 4 of the Cost Engineering Classification System.[25] Starting with estimations of high throughput R2R equipment costs needed for realizing a high efficiency single junction ST-OPV structure, we estimate the maintenance, utility, labor and materials costs. We further estimate costs due to the inclusion of a microinverter for making the solar output compatible with most in-building ac electrical systems. Inclusion of the inverter significantly simplifies power window installation,[26] but is counterbalanced by the added cost of the inverter. Assuming the PV modules are integrated within double-pane windows to simplify encapsulation, we expect a manufacturing cost of \$106.16/m^2. This places a premium on the average double-pane window cost in U.S. of \$106.80/m^2[27]–[29] including the sealant, frame and assembly costs, based on market data and assuming a 30% margin. We estimate the cost can be as low as \$57.24/m^2, provided that the materials and inverter costs can be incrementally reduced. We assume a base case semitransparent module *PCE* = 10%, which compares with current non-transparent module *PCE* > 14%.[13] With *GFF* = 70%, and an inverter efficiency of η_{inv} = 95%, the estimated module cost without the inverter is \$0.68/W$_p$, at ~160MW annual production volume. We estimate a microinverter cost of \$0.78/W$_p$ based on market data, which is similar to the household scale Si PV microinverter cost of \$0.45/W$_p$[30] considering the efficiency differences between the two PV technologies. Assuming modest cost reductions in microinverters, OPV materials, contacts and optical coatings, we estimate the total system cost including miscellaneous costs can be further reduced from \$1.6/W$_p$ to \$0.47/W$_p$ in the foreseeable the future. This suggests an energy payback period of 2 to 6 years depending on the window orientation, local cost of electricity, and location of installation.

II. Cost estimate assumptions and results

We divide the manufacturing cost into four categories – capital equipment, labor, utilities and materials. Additional miscellaneous costs including marketing, general and administrative (G&A), research and development (R&D) are assumed to be 10% of total manufacturing cost based on recent 3-year average of PV manufacturing industry standards.[31] Then, the desired OPV module structure for cost analysis is chosen and performance assumptions are established. For this analysis, we assume a 1 m wide R2R manufacturing web for PV module fabrication. Figure 2(a) shows a schematic of an archetype semitransparent OPV cell structure. Starting from flexible barrier substrate, the first deposited layer is the transparent cathode, followed by the cathode buffer/exciton blocking layer, active layer, anode buffer, and transparent anode. The layers are encapsulated by a second barrier substrate. For transparency, a mixture of non-fullerene acceptors and energy-level-matched donors that selectively absorb near-infrared (IR) photons are used as the active layer.[32]–[36] Optical layers for outcoupling the visible and reflecting the IR photons are included to increase efficiency and transparency.[15]

A conceptual, schematic top view of a ST-OPV module integrated into a 1 m × 2 m window used in our cost estimates is shown in Fig. 2(b). An array of 2 cm × 2 cm ST-OPV cells are connected in a series-parallel circuit within the window module. Electrical interconnects and a microinverter for each module are integrated outside the viewing space of the window. The transparent PV cell foils can be directly attached onto a single-pane window surface without additional encapsulation,[4], [37] or they can be inserted into the pocket of a double-pane window[38] as shown in Fig. 3. In this analysis, we use the latter configuration since it allows for simplified OPV encapsulation with inert gas commonly used within the gap between the panes. The optical coupling layers can be separately deposited onto the inner surfaces of the opposite panes. Integration of the optical coupling layers with the PV module itself is simplified compared to the direct attachment onto a single-pane window, which requires deposition of all layers onto the substrate film, or integration with the encapsulating lid.

Figure 4 shows materials choices and manufacturing processes used in the study. Starting from an ITO-coated transparent PET substrate, the bottom contact is patterned by laser scribing. The ZnO cathode buffer/exciton blocking layer, PTB7-Th:BT-CIC active layer, and MoO_3 anode buffer are consecutively applied via slot-die coating. Each solution process is followed by solvent annealing in an oven integrated within the R2R tool. Before top contact deposition, the active layer is patterned for interconnect attachment using laser scribing. Contact layers are patterned during printing and sputtering and do not require additional scribing. The roll is transferred into a vacuum chamber for thin Ag transparent top contact[15] R2R sputter deposition. After contact patterning, the roll is encapsulated by attachment of a second barrier substrate, spliced into the desired size, laminated onto a glass pane, and assembled into the double pane window.

A list of required manufacturing equipment and their annual costs assuming 10 year linear depreciation is summarized in Table II. Here, we assume a 10 year equipment lifetime, although depreciation rates of 5 to 7 years are often used to maximize financial efficiency (i.e. to reduce soft costs due to tax adjustments, etc.).[39], [40] An accurate plant cost estimate depends on location and total area. For our estimate, therefore, we simply assume a plant cost of four times the total equipment cost, with an additional 10% contingency for waste handling.[22], [41] The machine platform comprises a skeletal support structure and R2R web manipulation components including rollers, tensioning systems, motors, etc. Printing and slot-die coating stations include baking ovens for thermal annealing the films after coating. Scribing and test/sort equipment costs were estimated by proportionally scaling the lamination station cost.[23] Assumptions for labor, utilities cost and production parameters are provided in Table III. A 5 m/min roll translation speed during deposition ensures stable thickness and quality control of each layer.[23], [39], [40] Considering a 1 m web width and 5% roll preparation time during the manufacturing cycle, the annual PV module production area is 2.25×10^6 m^2, assuming 11 month/yr and 24 h/day utilization. This production rate corresponds to ~160MW/year production, assuming a base case module performance of $GFF = 70\%$, $\eta_{\mathrm{inv}} = 95\%$ and $PCE = 10\%$, which is consistent with recent advances in ST-OPV efficiency of nearly 11%[14] and a reported opaque OPV module efficiency of 14%.[13] Here, $GFF = 70\%$ is a conservative estimate that allows room for inter-cell contacts, and window structures outside of the viewing area. We also assume one unskilled personnel per each lamination, splicing and scribing station, and one skilled personnel per each coating and printing station, resulting in a total of 6 unskilled labor and 5 skilled labor per production line. With 55% employee benefits, \$15/h and \$20/h unskilled and skilled wages, the annual labor costs are \$1.2MM and \$1.3MM, respectively. As our estimate is not at a stage to confirm detailed manpower cost such as marketing, human resources, legal or financial cost, the marketing and selling costs are included in the 10% miscellaneous cost. Additional labor might be required when detailed manpower structures are confirmed. We include electricity costs of \$83K/year for sputtering and \$44K/year for coating and printing utilities support based on estimated power consumption and an industrial electricity costs of \$0.07/kWh.[42] Lamination, splicing and testing/sorting stations are assumed to use half the power of the coating and printing stations. Additional utilities costs such as process chilled water are \$100K/system/year. Maintenance of \$10K/year is assumed for each station.

With these assumptions, the manufacturing cost is calculated by dividing the total cost for annual production by the area produced, as listed in Table IV. Materials costs for each layer is the product of the amount of material required, and the source material cost based on weight, We assume 80% material utilization efficiency for solution processed layers, and 25% for sputtered layers.[39], [40] Since active layer materials costs are unavailable in volume quantities, we estimate the bulk organic semiconductor cost based on \$31/g/synthesis step, times number of steps required.[43] A three-step synthesis of PTB7-Th,[44] five-step synthesis of BT-CIC[32], [33] for a PTB7-Th:BT-CIC 1:1.5 mixture results in \$130.2/g. Using the density of the mixture after annealing, an active layer thickness of 160 nm, we obtain \$29.67/m^2 for the active layer materials. Materials cost estimates for ITO on PET, barrier substrates, ZnO, MoO_3, and Ag are provided in SI, Table I.

The optical coating structure depends on the location and orientation of the installation. We estimate the cost of the coating by subtracting the cost of glass without coating (\$3/m^2), from the cost of glass with an anti-reflective coating (\$7/m^2).[45] A microinverter is required to combine the outputs of several photovoltaic modules into the ac power line of the building to compensate for non-uniform solar illumination on each module[26]. For a 2 m × 1 m module comprising an array of series and parallel connected 2 cm × 2 cm cells, each with an open circuit voltage of 0.7 V and short circuit current of 16 mA/cm^2 for APT = 50%,[15] we estimate a 16 Adc and 34 Vdc maximum module output. We use an inverter price of \$52/m^2 estimated by applying a 20% bulk purchase discount from commercial price.[46] With an additional 10% miscellaneous cost premium, we arrive at a total module cost estimate of \$48.96/m^2 and \$106.16/m^2 without and with the inverter, respectively.

Although our materials cost estimates are as realistic as possible at this time, we nevertheless expect a ±30% error for active layer and optical layer coatings, considering the lack of information on bulk-production active layer materials cost, and location and orientation dependence of the window. We expect a potential ±20% error for other PV layers due to cost variations between different vendors, and the expected purchase volume. A sensitivity chart according to the estimated errors is shown in SI, Fig. 1.

III. Discussion

Our analysis indicates that materials cost comprises ~90% of total PV module manufacturing cost. This result agrees with previous analyses normalized to our production levels that indicate the material costs are dominant, accounting for 90-98% of total module cost [20]–[24]. Due to high R2R system throughput, the fixed costs scale inversely, whereas material and microinverter costs scale linearly with the area produced. Indeed, this conclusion is consistent with other volume-manufactured PV technologies where materials are found to consume a large fraction of the total system cost.[30], [45], [47], [48] The production of 160 MW/year can lead to additional costs for handling and warehousing; considerations needed to refine future cost estimates.

Figure 5(a) shows a potential scenario in materials cost reduction without including the 10% miscellaneous cost contribution. The most expensive device component is its active layer due to its thickness, and the several steps used in materials synthesis. If the materials require only a 2-step synthesis, the materials cost can be reduced by 38%. The ITO on PET anode and the optical coating are the next most expensive contributions. This suggests that development of cost-effective, flexible and transparent contacts is an important challenge to be met for reducing ST-OPV costs. With the assumption of 50% future reduction in the bottom contact, optics and barrier substrate costs, the total materials cost is reduced by additional 11%. PV glass cost including the module, inverter and miscellaneous costs compared with double-pane windows[27]–[29] is shown in Fig.

5(b). Initial estimates suggest that PV glass is approximately twice as expensive as an average double-pane window. With modestly improved cost efficiencies, the additional cost from PV module integration can be only ~60% of average, uninstalled windows cost. Another important factor to consider is that double-pane windows are priced between $50/m^2 – $200/m^2, from low-end to high-end models.[27]–[29] Considering that power generating windows will be positioned as high-end products, the PV module cost can range from 33% to as low as 25% of the total installed power generating window cost.

The module cost including the microinverter is shown in Fig. 6. Additional simplifications in materials synthesis and a 50% reduction in microinverter costs changes the module cost from a base case of $1.6/W$_p$, to $1.16/W$_p$. Provided that ST-OPV lab efficiency is increased to yield a module *PCE* = 15% and *GFF* = 90%, the cost further reduces to $0.47/W$_p$. These realistic improvements in performance in the near future suggest that the production cost of ST-OPVs can be on par with Si photovoltaics.[30]

To estimate the economic feasibility of ST-OPV windows, we simulate annual power generation from a BIPV module with *PCE*=15%, *GFF*=90% using the PV-GIS tool[49] in multiple regions across the U.S., from latitudes 27° to 48°. For comparison, a calculation based on the annual solar path assuming uniform, AM 1.5G solar irradiance of 800W/m^2 is also provided to show the latitude dependence without effects of weather or altitude of different locations.[47]

Five different configurations were modelled: east and south facing windows, east and south facing 45° tilted surfaces, and the optimal orientation determined by the PV-GIS tool. The data points in Fig. 7 show the estimate based on annual solar irradiance data, whereas dashed lines show calculation based on uniform irradiance throughout the year. Bars centered at each data point allow for variants in altitude differences within the regions at the same latitude.

There is only a small dependence of annual power generation on latitude for south facing, 45° tilted surfaces, and east facing windows. East facing 45° tilted surfaces show a monotonic decrease, and south facing windows show an increase of power generation with increasing latitude. With the module cost estimate of $55.52/m^2, and a typical residential electricity cost of $0.13/kWh,[42] the payback period of the ST-OPV window module ranges from 2 to 6 years, depending on the location and orientation of the installation.

IV. Conclusion

Our study of the manufacturing cost for ST-OPV modules used in power generating windows suggests that high throughput R2R manufacturing can potentially enable large scale production of economically feasible and visually attractive building applied solar harvesting appliances. A principal conclusion of our analysis is that materials and microinverter costs are the dominant contributors to total module cost, significantly overtaking the costs of equipment and other miscellaneous operational costs. Starting from \$1.6/W_p estimate based on current ST-OPV performance, we expect the cost could be as low as \$0.47/W_p with modest future improvements in module performance and production cost reductions. When used in high end, double-pane thermally insulating windows, we anticipate an average energy payback period of 2 to 6 years, depending on the location, window orientation and local electricity cost of the installation.

Acknowledgements

We thank Dr. Pavinatto at University of Washington and Mr. Campbell at Ångstrom engineering for fruitful discussion on roll to roll system designs and cost. This material is based upon work supported by the U.S. Department of Energy's Office of Energy Efficiency and

Renewable Energy (EERE) under the Solar Energy Technology Office (SETO) Award Number DE-EE0008561. This report was prepared as an account of work sponsored by an agency of the United States Government. Neither the United States Government nor any agency thereof, nor any of their employees, makes any warranty, express or implied, or assumes any legal liability or responsibility for the accuracy, completeness, or usefulness of any information, apparatus, product, or process disclosed, or represents that its use would not infringe privately owned rights. Reference herein to any specific commercial product, process, or service by trade name, trademark, manufacturer, or otherwise does not necessarily constitute or imply its endorsement, recommendation, or favoring by the United States Government or any agency thereof. The views and opinions of authors expressed herein do not necessarily state or reflect those of the United States Government or any agency thereof. The authors also thank Universal Display Corp. for partial support of this work.

Conflict of interest

One of the authors (SRF) holds an equity interest in one of the sponsors of this work (UDC). This apparent conflict is under management by the University of Michigan Office of Research.

References

[1] P. Heinstein, C. Ballif, and L. E. Perret-Aebi, "Building integrated photovoltaics (BIPV): Review, potentials, barriers and myths," *Green*, vol. 3, no. 2. Walter de Gruyter GmbH, pp. 125–156, 2013.

[2] R. J. Yang and P. X. W. Zou, "Building integrated photovoltaics (BIPV): costs, benefits, risks, barriers and improvement strategy," *Int. J. Constr. Manag.*, vol. 16, no. 1, pp. 39–53, Jan. 2016.

[3] M. A. Alim *et al.*, "Is it time to embrace building integrated Photovoltaics? A review with particular focus on Australia," *Solar Energy*, vol. 188. Elsevier Ltd, pp. 1118–1133, 01-Aug-2019.

[4] A. K. Shukla, K. Sudhakar, and P. Baredar, "Recent advancement in BIPV product technologies: A review," *Energy and Buildings*, vol. 140. Elsevier Ltd, pp. 188–195, 01-Apr-2017.

[5] H. Gholami, H. N. Røstvik, and D. Müller-Eie, "Holistic economic analysis of building integrated photovoltaics (BIPV) system: Case studies evaluation," *Energy Build.*, vol. 203, Nov. 2019.

[6] F. Cucchiella and I. Dadamo, "Estimation of the energetic and environmental impacts of a roof-mounted building-integrated photovoltaic systems," *Renewable and Sustainable Energy Reviews*, vol. 16, no. 7. pp. 5245–5259, Sep-2012.

[7] T. James, A. Goodrich, M. Woodhouse, R. Margolis, and S. Ong, "Building-Integrated Photovoltaics (BIPV) in the Residential Sector: An Analysis of Installed Rooftop System Prices," Golden, CO (United States), Nov. 2011.

[8] B. Joseph, T. Pogrebnaya, and B. Kichonge, "Semitransparent Building-Integrated Photovoltaic: Review on Energy Performance, Challenges, and Future Potential," *International Journal of Photoenergy*, vol. 2019. Hindawi Limited, 2019.

[9] B. Van Der Wiel, H. J. Egelhaaf, H. Issa, M. Roos, and N. Henze, "Market readiness of organic photovoltaics for building integration," *Twentieth-Century Music*, vol. 1639, no. 1, Nov. 2014.

[10] M. J. Sorgato, K. Schneider, and R. Rüther, “Technical and economic evaluation of thin-film CdTe building-integrated photovoltaics (BIPV) replacing façade and rooftop materials in office buildings in a warm and sunny climate,” *Renew. Energy*, vol. 118, pp. 84–98, Apr. 2018.

[11] Q. Burlingame, X. Huang, X. Liu, C. Jeong, C. Coburn, and S. R. Forrest, “Intrinsically stable organic solar cells under high-intensity illumination,” *Nature*, vol. 573, no. 7774. Nature Publishing Group, pp. 394–397, 19-Sep-2019.

[12] Y. Lin *et al.*, “17% Efficient Organic Solar Cells Based on Liquid Exfoliated WS $_2$ as a Replacement for PEDOT:PSS,” *Adv. Mater.*, vol. 31, no. 46, p. 1902965, Nov. 2019.

[13] S. Dong *et al.*, “Single-Component Non-halogen Solvent- Processed High-Performance Organic Solar Cell Module with Efficiency over 14 % Single-Component Non-halogen Solvent-Processed High-Performance Organic Solar Cell Module with Efficiency over 14 %,” *Joule*, pp. 1–13, 2020.

[14] Y. Li *et al.*, “Color-Neutral, Semitransparent Organic Photovoltaics,” *Proc. Natl. Acad. Sci. U. S. A.*, vol. In Press, 2020.

[15] Y. Li *et al.*, “Enhanced Light Utilization in Semitransparent Organic Photovoltaics Using an Optical Outcoupling Architecture,” *Adv. Mater.*, vol. 31, no. 40, p. 1903173, Oct. 2019.

[16] C. J. Traverse, R. Pandey, M. C. Barr, and R. R. Lunt, “Emergence of highly transparent photovoltaics for distributed applications,” *Nature Energy*, vol. 2, no. 11. Nature Publishing Group, pp. 849–860, 01-Nov-2017.

[17] F. C. Krebs *et al.*, “A complete process for production of flexible large area polymer solar cells entirely using screen printing-First public demonstration,” *Sol. Energy Mater. Sol. Cells*, vol. 93, no. 4, pp. 422–441, Apr. 2009.

[18] R. Søndergaard, M. Hösel, D. Angmo, T. T. Larsen-Olsen, and F. C. Krebs, “Roll-to-roll fabrication of polymer solar cells Open access under CC BY-NC-ND license,” 2012.

[19] R. R. Søndergaard, M. Hösel, and F. C. Krebs, “Roll-to-Roll fabrication of large area functional organic materials,” *Journal of Polymer Science, Part B: Polymer Physics*, vol. 51, no. 1. John Wiley & Sons, Ltd, pp. 16–34, 01-Jan-2013.

[20] B. Azzopardi, C. J. M. Emmott, A. Urbina, F. C. Krebs, J. Mutale, and J. Nelson, “Economic assessment of solar electricity production from organic-based photovoltaic modules in a domestic environment,” *Energy Environ. Sci.*, vol. 4, no. 10, pp. 3741–3753, 2011.

[21] F. Machui *et al.*, “Cost analysis of roll-to-roll fabricated ITO free single and tandem organic solar modules based on data from manufacture,” *Energy Environ. Sci.*, vol. 7, no. 9, pp. 2792–2802, Aug. 2014.

[22] C. J. Mulligan *et al.*, “A projection of commercial-scale organic photovoltaic module costs,” *Sol. Energy Mater. Sol. Cells*, vol. 120, no. PART A, pp. 9–17, 2014.

[23] J. Guo and J. Min, “A Cost Analysis of Fully Solution-Processed ITO-Free Organic Solar Modules,” *Adv. Energy Mater.*, vol. 9, no. 3, pp. 1–9, 2019.

[24] A. Gambhir, P. Sandwell, and J. Nelson, “The future costs of OPV – A bottom-up model of material and manufacturing costs with uncertainty analysis,” *Sol. Energy Mater. Sol. Cells*, vol. 156, pp. 49–58, Nov. 2016.

[25] P. Christensen *et al.*, “18R-97: Cost Estimate Classification System - As Applied in Engineering, Procurement, and Construction for the Process Industries,” 2005.

[26] H. P. Ikkurti and S. Saha, “A comprehensive techno-economic review of microinverters for Building Integrated Photovoltaics (BIPV),” *Renew. Sustain. Energy Rev.*, vol. 47, pp. 997–1006, Jul. 2015.

[27] “Window Glass Replacement Cost | Window Pane Replacement Prices.” [Online]. Available: https://www.fixr.com/costs/window-glass-replacement. [Accessed: 02-Jun-2020].

[28] “How much does it cost to replace a window glass?” [Online]. Available: https://howmuch.net/costs/window-glass-replacement. [Accessed: 02-Jun-2020].

[29] “2020 Cost of Broken Window Repair - Estimates and Prices Paid.” [Online]. Available: https://home.costhelper.com/window-repair.html. [Accessed: 02-Jun-2020].

[30] R. Fu, D. Feldman, and R. Margolis, “U.S. Solar Photovoltaic System Cost Benchmark:

Q1 2018," 2018.

[31] "First Solar, Inc. - Financials - Annual Reports." [Online]. Available: https://investor.firstsolar.com/financials/annual-reports/default.aspx. [Accessed: 02-Jun-2020].

[32] Y. Li *et al.*, "A near-infrared non-fullerene electron acceptor for high performance polymer solar cells," *Energy Environ. Sci.*, vol. 10, no. 7, pp. 1610–1620, Jul. 2017.

[33] Y. Li *et al.*, "High Efficiency Near-Infrared and Semitransparent Non-Fullerene Acceptor Organic Photovoltaic Cells," *J. Am. Chem. Soc.*, vol. 139, no. 47, pp. 17114–17119, Nov. 2017.

[34] F. Liu *et al.*, "Efficient Semitransparent Solar Cells with High NIR Responsiveness Enabled by a Small-Bandgap Electron Acceptor," *Adv. Mater.*, vol. 29, no. 21, p. 1606574, Jun. 2017.

[35] S. Chen *et al.*, "A Nonfullerene Semitransparent Tandem Organic Solar Cell with 10.5% Power Conversion Efficiency," *Adv. Energy Mater.*, vol. 8, no. 31, p. 1800529, Nov. 2018.

[36] Y. Cui *et al.*, "Efficient Semitransparent Organic Solar Cells with Tunable Color enabled by an Ultralow-Bandgap Nonfullerene Acceptor," *Adv. Mater.*, vol. 29, no. 43, p. 1703080, Nov. 2017.

[37] B. Van Der Wiel, H.-J. Egelhaaf, H. Issa, M. Roos, and N. Henze, "Market Readiness of Organic Photovoltaics for Building Integration," *Mater. Res. Soc. Symp. Proc*, vol. 1639, 2020.

[38] N. Skandalos and D. Karamanis, "PV glazing technologies," *Renewable and Sustainable Energy Reviews*, vol. 49. Elsevier Ltd, pp. 306–322, 16-May-2015.

[39] "Private communication, Angstrom Engineering." 2020.

[40] "Private communication, FOM Technology." 2020.

[41] M.S. Peters, K.D. Timmerhaus, and R.E. West, *Plant design and economics for chemical engineers*, Fifth ed. New York, USA: McGraw-Hill Publishing, 2003.

[42] U.S. Energy Information Administration, “Average price of electricity to ultimate customers by end-use sector.” [Online]. Available: https://www.eia.gov/electricity/monthly/epm_table_grapher.php?t=epmt_5_6_a. [Accessed: 25-Apr-2020].

[43] T. P. Osedach, T. L. Andrew, and V. Bulovi´cbulovi´c, “Effect of synthetic accessibility on the commercial viability of organic photovoltaics †.”

[44] S. Zhang, L. Ye, W. Zhao, D. Liu, H. Yao, and J. Hou, “Side chain selection for designing highly efficient photovoltaic polymers with 2D-conjugated structure,” *Macromolecules*, vol. 47, no. 14, pp. 4653–4659, Jul. 2014.

[45] K. A. W. Horowitz, R. Fu, and M. Woodhouse, “An analysis of glass-glass CIGS manufacturing costs,” *Sol. Energy Mater. Sol. Cells*, vol. 154, pp. 1–10, Sep. 2016.

[46] “Enphase Store Enphase Microinverters.” [Online]. Available: https://store.enphase.com/storefront/en-us/microinverters?_ga=2.216323988.347453585.1599417251-993301144.1599417251. [Accessed: 08-Jul-2019].

[47] K. A. Horowitz, T. W. Remo, B. Smith, and A. J. Ptak, “A Techno-Economic Analysis and Cost Reduction Roadmap for III-V Solar Cells,” *NREL/TP-6A20-72103*, 2018. [Online]. Available: http://www.osti.gov/servlets/purl/1484349/. [Accessed: 03-Sep-2019].

[48] B. Lee, D. Fan, and S. R. Forrest, “A high throughput, linear molecular beam epitaxy system for reduced cost manufacturing of GaAs photovoltaic cells: Will GaAs ever be inexpensive enough?,” *Sustain. Energy Fuels*, vol. 4, no. 4, pp. 2035–2042, Apr. 2020.

[49] “Photovoltaic Geographical Information System (PVGIS) | EU Science Hub.” [Online]. Available: https://ec.europa.eu/jrc/en/pvgis. [Accessed: 31-Mar-2020].

Table I. Recent advances in semitransparent OPV performance

Active layer	J_{sc} (mA/cm^2)	V_{oc} (V)	FF	PCE (%)	APT* (%)	LUE (%)	Reference
PTB7-Th : IEICO-4Cl	17.6	0.714	0.554	6.97	38	2.65	[36]
PTB7-Th : BT-CIC	15.8	0.68	0.662	7.10	39	2.75	[33]
PTB7-Th : IEICS-4F	16.97	0.72	0.58	7.20	34	2.44	[35]
PTB7-Th : ATT-2	17.23	0.71	0.57	7.02	32	2.25	[34]
PTB7-Th : BT-CIC : TTFIC	16.6	0.68	0.72	8.00	44	3.56	[15]
PTB7-Th : A078	20.4	0.75	0.70	10.8	45.7	5.0	[14]

*APT recalculated from the literature if possible, otherwise AVT was used.

Table II. Required equipment and plant cost estimate for manufacturing[(a)]

Item	Required quantity	Depreciation ($/year)	Reference
Machine platform	1	183K	[40]
Slot-die coating station	3	209K	[40]
Sputtering station	1	178K	[39]
Splice table	1	10K	[40]
Laminating station	2	25K	[40]
Laser scribing	2	75K	[40], [23]
Test / sort equipment	1	25K	[40],[23]
Plant cost	-	5.1MM	[22],[40]

(a) Plant cost is assumed to be 4 times the total equipment cost, with additional 10% for waste handling.

Table III. Assumptions for cost of ownership estimates

Item	Unit	Value
Roll moving speed	m/hr	300
Roll preparation and loading time	hr/hr	0.05
Substrate width	m	1
Production area per system	m^2/year/system	2.25MM
Unskilled labor	/system	6
Skilled labor	/system	5
Unskilled wage	$/system/year	$1.2MM
Skilled wage	$/system/year	$1.3MM
Electricity – Sputter[(a)]	$/equipment/year	$83K
Electricity – Coating / Printing station[(b)]	$/equipment/year	$44K
Utilities – Process chilled water, etc.	$/system/year	$100k
Maintenance	$/equipment/year	$10K
Maintenance time	month/year	1

(a) From refs. [38],[40]

(b) From refs. [39],[40]

Table IV. Itemized manufacturing cost estimates, in $\$/m^2$

Layer	Equipment/plant	Utilities	Labor	Materials	Inverter	Total
Plant cost	2.24	0	0	0	0	2.24
Machine platform	0.08	0.02	0.09	0	0	0.19
ITO on PET substrate	0	0	0	5.00	0	5.00
ZnO Cathode buffer	0.09	0.02	0.12	0.02	0	0.25
PTB7-Th : BT-CIC Active layer	0.09	0.02	0.12	29.67	0	29.89
MoO_3 Anode buffer	0.09	0.02	0.12	0.03	0	0.26
Ag Top contact	0.08	0.04	0.12	0.13	0	0.37
Top barrier substrate	0	0	0	1.5	0	1.5
Lamination	0.02	0.03	0.17	0.09	0	0.31
Splicing / Scribing	0.09	0.04	0.26	0	0	0.39
Testing / sorting	0.01	0.01	0.09	0	0	0.11
Optics	0	0	0	4	0	4.00
Inverter	0	0	0	0	52	52.00
Total[(a)]	2.78	0.23	1.07	40.43	52	96.51

(a) Values shown in the table are before an additional 10% miscellaneous cost is added.

Figure captions

Figure 1: Compilation of light utilization efficiency (*LUE*) vs. average photopic transmittance (*APT*) of semitransparent photovoltaic cells with different technologies. Data adapted from Refs. [15], [16]. APT is recalculated from literature when possible, otherwise the reported average visible transmittance (AVT) is used.

Figure 2: A schematic of an (a) archetype semitransparent OPV device structure, and (b) proposed PV module layout for window integration. The microinverter (μ-inverter) is positioned outside of the viewing area, and individual cells are laid out in a series-parallel array configuration.

Figure 3: Illustration of ST-OPV integrated onto windows. (Left) The PV module is laminated onto a single pane, and (right) into the pocket between a double pane, thermally insulating window. Typically, inert gas fills the gap between the panes.

Figure 4: Process sequence for manufacturing power generating modules comprising organic ST-OPVs and a double pane window.

Figure 5: Waterfall diagrams showing (a) materials cost in manufacturing ST-OPV modules with the impacts of several cost reduction scenarios, and (b) total PV glass cost including the window panes and the impacts of several cost reduction scenarios.

Figure 6: Waterfall diagram showing module and inverter cost in $/W$_p$ and the impacts of several cost reduction scenarios based on projected modest device performance improvements described in text

Figure 7: Simulated annual power generation from ST-OPV windows vs. latitude. The calculations are shown for different module orientations, and are based on annual solar irradiance from the PV-GIS tool (data points), and based on uniform, AM1.5G, 800 W/m^2 (peak) solar irradiance (dashed lines). The vertical bars for each data point account for variations in average cloud cover and altitudes at different locations within a given latitude.

Figure 1

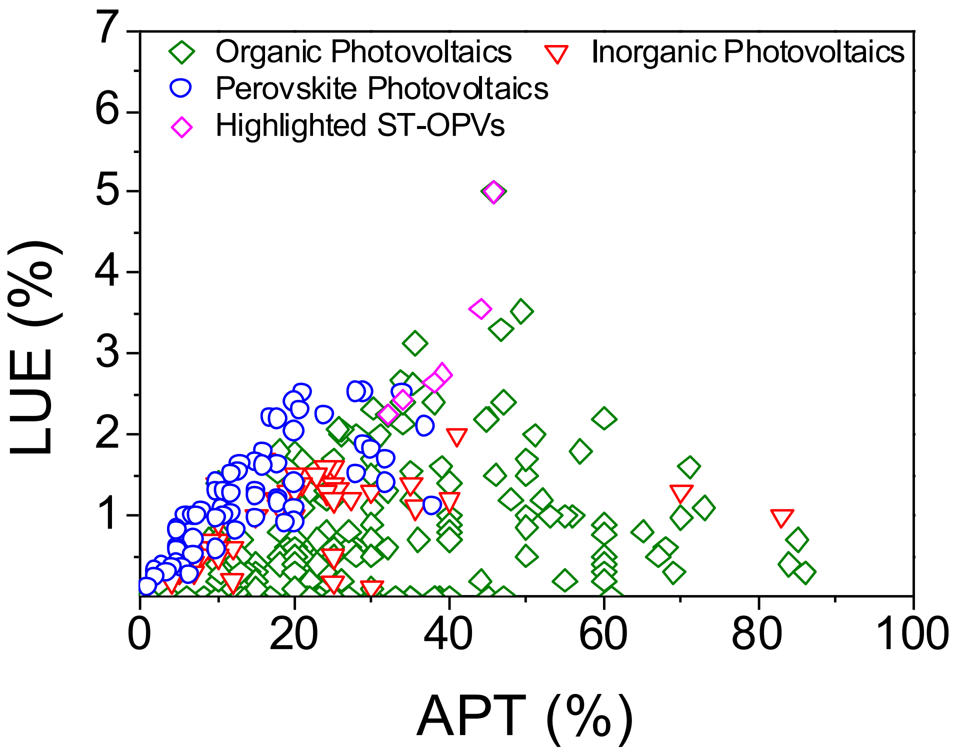
Organic Photovoltaics
Inorganic Photovoltaics
Perovskite Photovoltaics
Highlighted ST-OPVs
LUE (%)
APT (%)
0
1
2
3
4
5
6
7
0
20
40
60
80
100

Figure 2

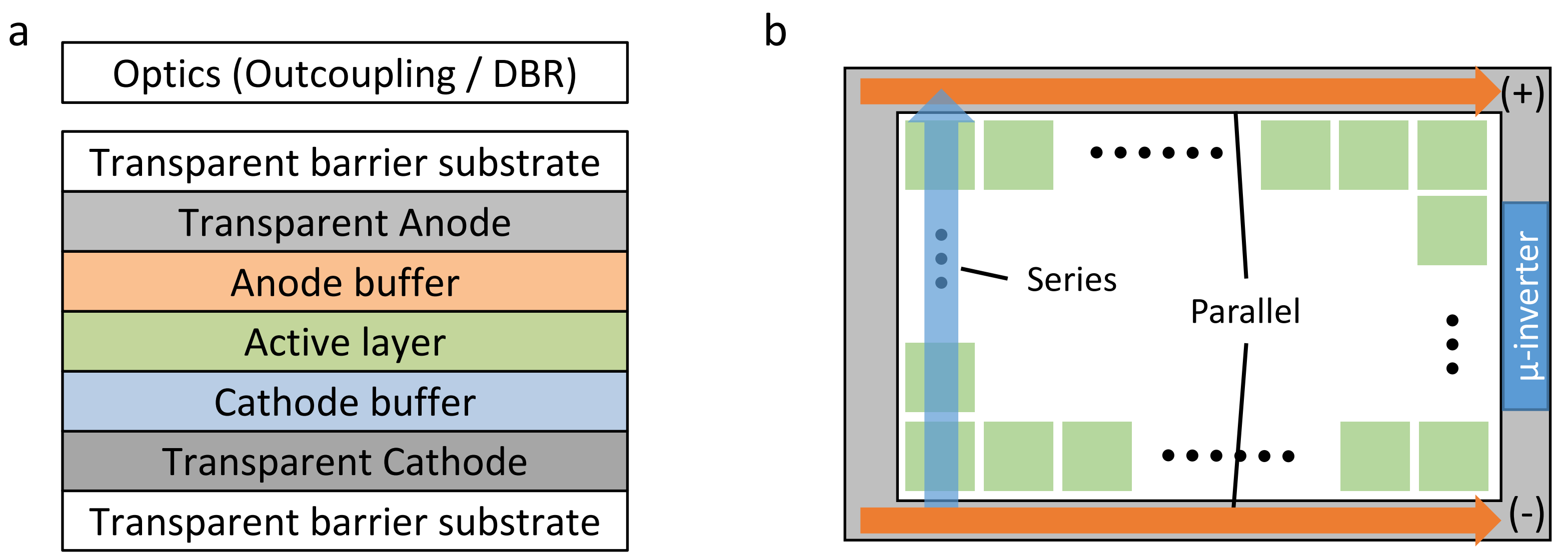
a
Optics (Outcoupling / DBR)
Transparent barrier substrate
Transparent Anode
Anode buffer
Active layer
Cathode buffer
Transparent Cathode
Transparent barrier substrate
b
(+)
Series
Parallel
µ-inverter
(-)

Figure 3

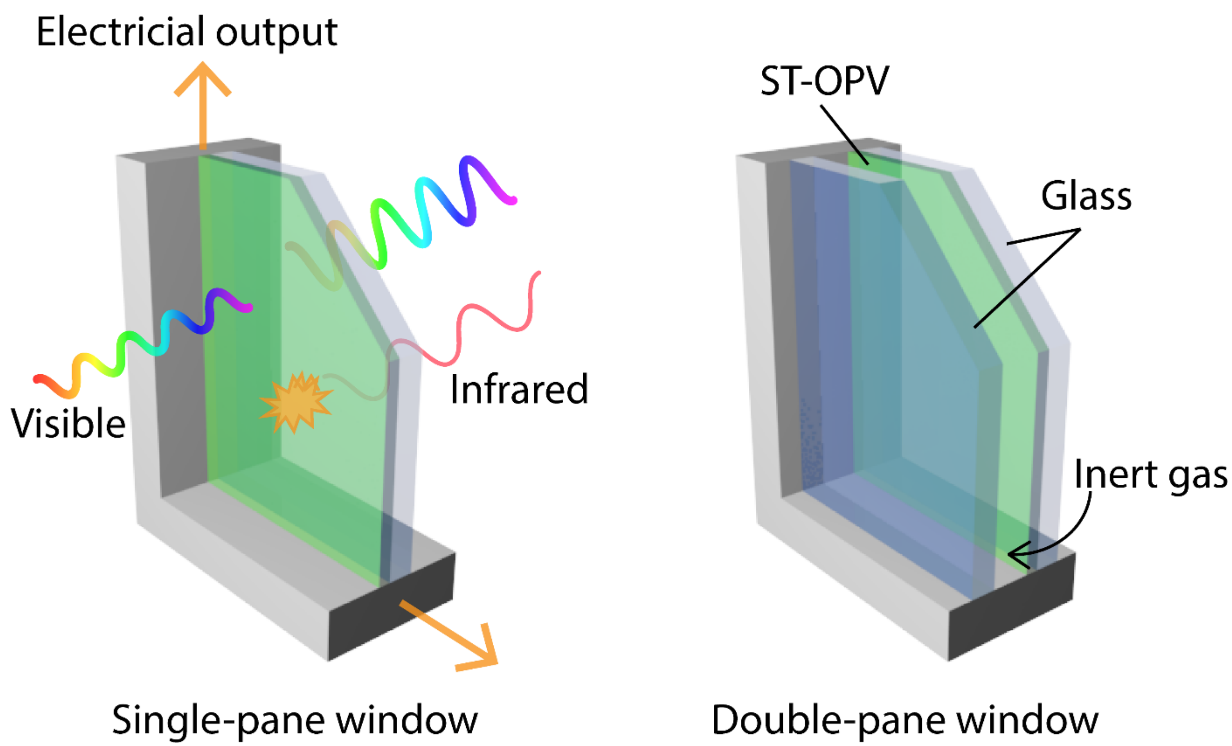
Electricial output
Visible
Infrared
Single-pane window
ST-OPV
Glass
Inert gas
Double-pane window

Figure 4

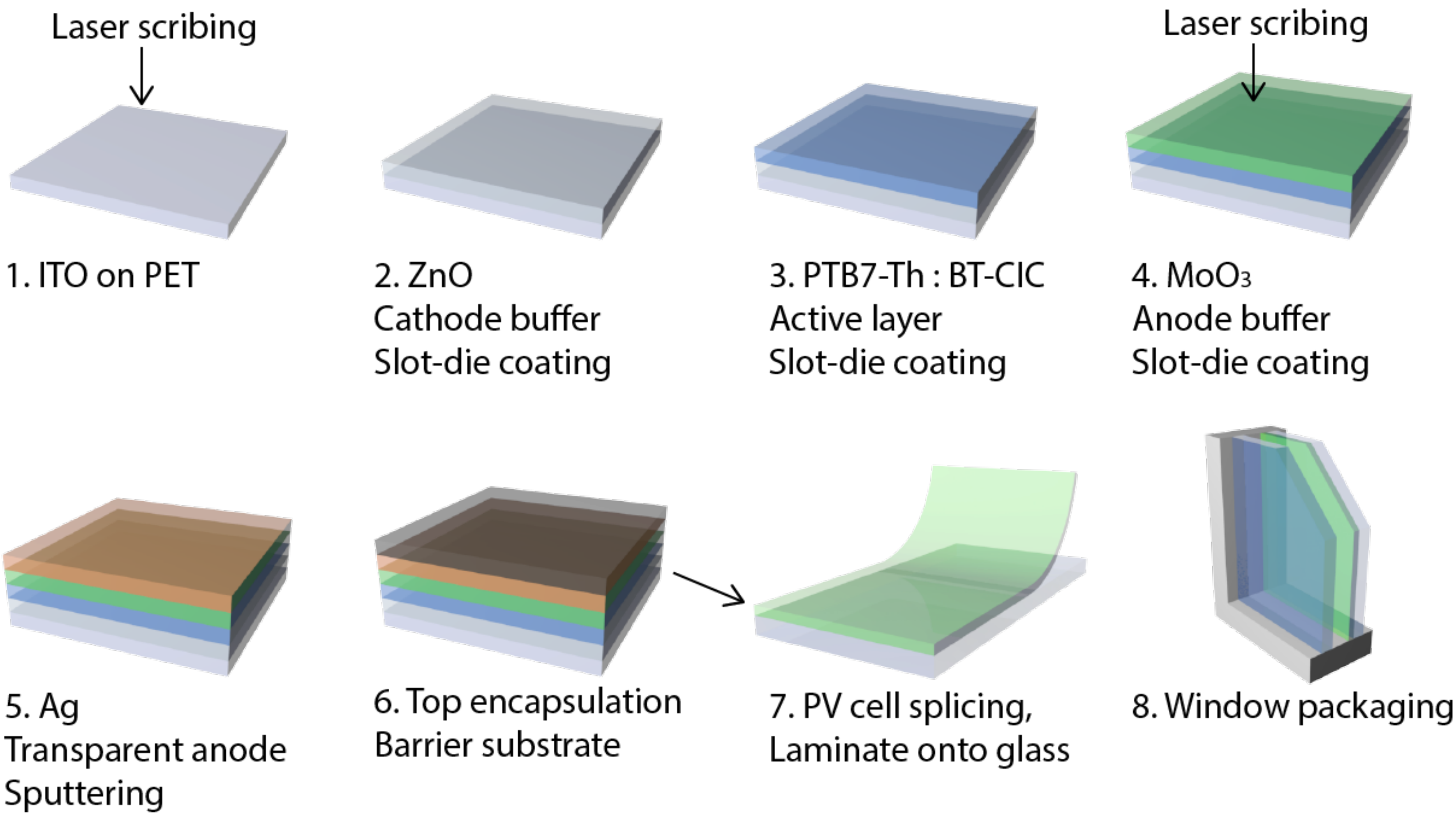
Laser scribing
Laser scribing
1. ITO on PET
2. ZnO
Cathode buffer
Slot-die coating
3. PTB7-Th : BT-CIC
Active layer
Slot-die coating
4. MoO3
Anode buffer
Slot-die coating
5. Ag
Transparent anode
Sputtering
6. Top encapsulation
Barrier substrate
7. PV cell splicing,
Laminate onto glass
8. Window packaging

Figure 5

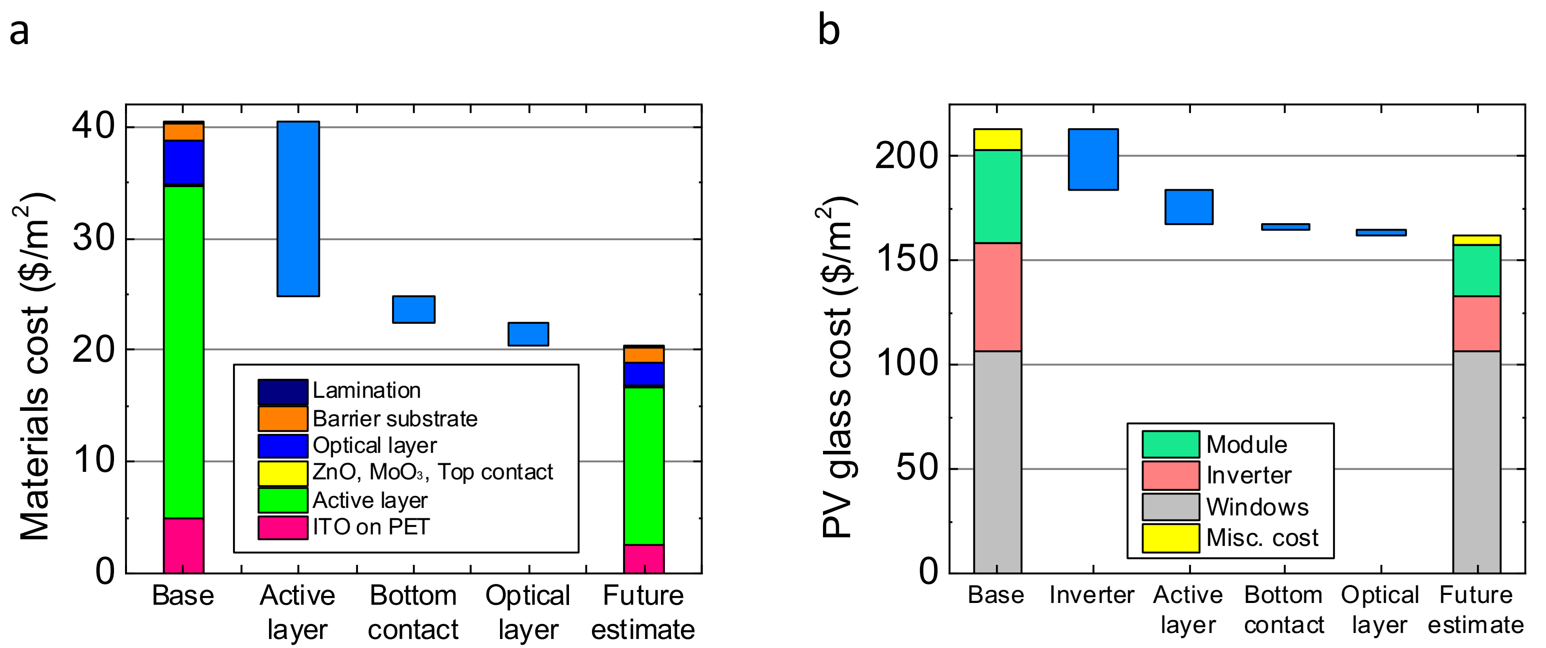
a
Materials cost ($/m^2)
0
10
20
30
40
Base
Active layer
Bottom contact
Optical layer
Future estimate
Lamination
Barrier substrate
Optical layer
ZnO, MoO₃, Top contact
Active layer
ITO on PET
b
PV glass cost ($/m^2)
0
50
100
150
200
Base
Inverter
Active layer
Bottom contact
Optical layer
Future estimate
Module
Inverter
Windows
Misc. cost

Figure 6

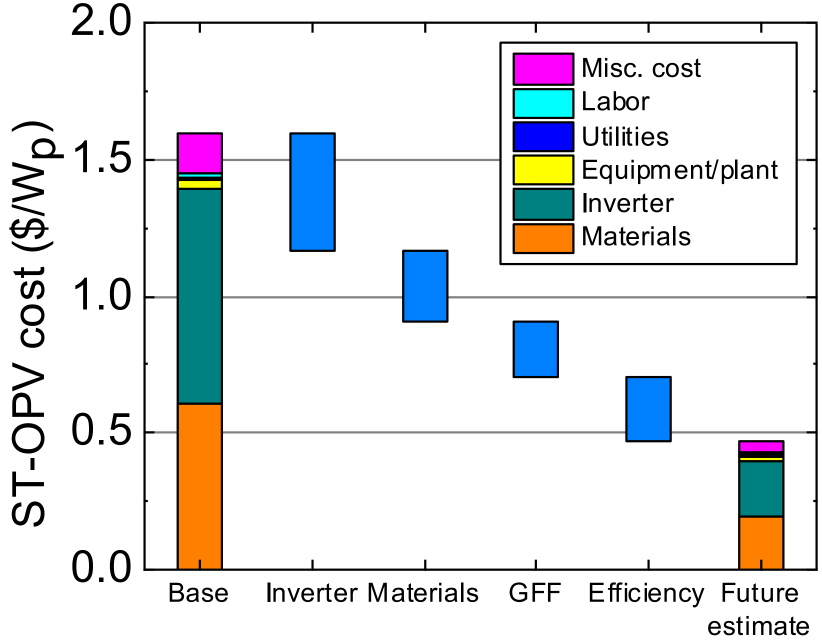
2.0
1.5
1.0
0.5
0.0
ST-OPV cost ($/W$_p$)
Misc. cost
Labor
Utilities
Equipment/plant
Inverter
Materials
Base
Inverter
Materials
GFF
Efficiency
Future estimate

Figure 7

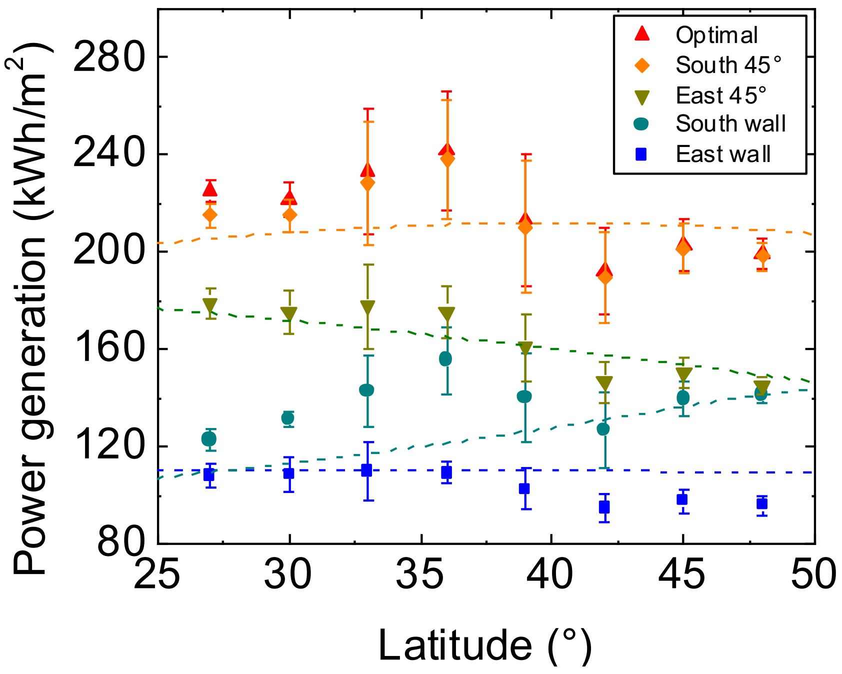
Optimal
South 45°
East 45°
South wall
East wall
Power generation (kWh/m²)
280
240
200
160
120
80
25
30
35
40
45
50
Latitude (°)